

Faraday Discussions

Accepted Manuscript



This manuscript will be presented and discussed at a forthcoming Faraday Discussion meeting. All delegates can contribute to the discussion which will be included in the final volume.

Register now to attend! Full details of all upcoming meetings: <http://rsc.li/fd-upcoming-meetings>



This is an *Accepted Manuscript*, which has been through the Royal Society of Chemistry peer review process and has been accepted for publication.

Accepted Manuscripts are published online shortly after acceptance, before technical editing, formatting and proof reading. Using this free service, authors can make their results available to the community, in citable form, before we publish the edited article. We will replace this *Accepted Manuscript* with the edited and formatted *Advance Article* as soon as it is available.

You can find more information about *Accepted Manuscripts* in the [Information for Authors](#).

Please note that technical editing may introduce minor changes to the text and/or graphics, which may alter content. The journal's standard [Terms & Conditions](#) and the [Ethical guidelines](#) still apply. In no event shall the Royal Society of Chemistry be held responsible for any errors or omissions in this *Accepted Manuscript* or any consequences arising from the use of any information it contains.

InfraRed Imaging of Small Molecules in Living Cells: from In Vitro Metabolic Analysis to Cytopathology

Luca Quaroni, Theodora Zlateva, Katia Wehbe, Gianfelice Cinque

Abstract

A major topic in InfraRed (IR) spectroscopic studies of living cells is the complexity of the vibrational spectra, involving hundreds of overlapping absorption bands from all the cellular components present at detectable concentrations. We focus on to the relative contribution of both small-molecule metabolites and macromolecules, while defining the spectroscopic properties of cells and tissue in the middle IR (midIR) region. As a consequence, we show the limitations of current interpretative schemes that rely on a small number of macromolecules for IR band assignment. The discussion is framed specifically around the glycolytic metabolism of cancer cells because of the potential pharmacological applications. Several metabolites involved in glycolysis by A549 lung cancer cells can be identified by this approach, which we refer to as Correlated Cellular Spectro-Microscopy (CSM). It is noteworthy that the rate of formation or consumption of specific molecules could be quantitatively assessed by this approach. We then extend this analysis to the two-dimensional case by performing IR imaging on single cells and cell clusters, detecting variations of metabolite concentration in time and space across the sample. The molecular detail obtained from this analysis allows its use in evaluating the pharmacological effect of inhibitors of glycolytic enzymes with potential consequences for in vitro drug testing. Finally we highlight the implications of the spectral contribution from cellular metabolites on applications in IR spectral cytopathology (SCP).

Introduction

Over the last twenty years IR spectromicroscopy has seen increasing applications in the study of cells and tissue because of its high sensitivity to molecular properties and its capability to perform a spatially resolved analysis of the sample. An IR absorption measurement can simultaneously provide information about the identity, concentration and biochemical properties of sample components. In spectromicroscopy the measurement can be performed on microscopic samples, including cells and tissue portions, with a spatial resolution which, in some optical configurations e.g. coupled to a Synchrotron Radiation (SR) source, is limited only by light diffraction.¹ IR mapping or imaging experiments provide the spatial distribution of molecules, without resorting to staining and, in principle, with minimal or no previous knowledge of sample composition. All these features have led to increased interest in using IR spectromicroscopy for the characterization of biological systems. The compositional sensitivity of IR absorption measurements has also generated enthusiasm about the diagnostic potential of the technique, leading to a new discipline that been termed spectral cytopathology (SCP). In SCP IR absorption spectra from biological samples are used to discriminate between healthy and pathological states by relying on the changes in molecular composition that accompany the onset of disease.²⁻⁶

An important development in the biological application of IR spectromicroscopy is its use to characterize biochemical reactions in living cells, using a combination of benchtop and synchrotron radiation sources. Early investigations in this field aimed at performing compositional studies of cells in an environment that ensures their viability⁷⁻¹³. In recent years this effort has further shaped itself into two broad directions. One direction of activity aims at

developing the competence to perform classical and quantitative biochemical experiments *in vivo*, such as kinetics, structure-function correlations and mechanistic studies.^{14 15-17} A different, although related, direction of activity aims at taking advantage of the broad sensitivity of IR absorption spectroscopy to study the activity of cells as a whole, such as in the quantitative description of metabolic networks.^{18, 19} Both directions share a common challenge in the need to identify and assign patterns of absorption bands amid the complexity of cellular IR absorption spectra.

To date the canonical approach to the interpretation of IR absorption spectra from biological samples follows a minimalistic scheme that reduces the spectrum to a combination of bands from a few classes of macromolecule families (proteins, polysaccharides, nucleic acids) plus acyl-containing lipids.²⁰ Developed during the early days of cellular IR studies, this scheme works as a general guide for the assignment of the most intense bands observed in tissue spectra.^{21, 22} Although very useful, it was pointed out early that such interpretation was a preliminary but not exhaustive approach, and it was suggested that more specific and detailed analysis should be performed in the context of each individual problem. Despite these cautionary notes, such minimalistic interpretation has become the standard approach for biological spectral analysis so far in IR literature. Reports that identified considerable contributions from other molecules in cellular IR spectra^{23, 24} did not substantially change this paradigm. Such neglect can be ascribed both to the relatively low spectral contribution of most individual molecular components other than the canonical ones (proteins, polysaccharides, nucleic acids, acyl lipids), to the difficulty in making reliable band assignments in the complex cellular environment, and to the low signal-to-noise ratio in spectromicroscopy measurements.

In an effort to clarify the spectral contribution of small molecules and to manage the problem of band assignment we have recently introduced a method called correlated cellular spectromicroscopy (CSM). The method relies on two-dimensional correlation spectroscopy (2D-COS) to identify clusters of bands belonging to the same molecule in a complex evolving system. The analysis identifies several bands from specific molecules allowing identification by spectral fingerprinting. CSM is suitable for real-time metabolomic analysis, including the measurement of rates of metabolite formation and consumption. Its application to the study of glycolysis in hypoxic A549 cells can detect several molecules associated to glycolysis.¹⁸

In this work we further develop the issues that led us to introduce CSM and discuss in general terms the role of small molecule metabolites in cellular IR absorption spectra. We want to show how a CSM analysis can be further integrated with 2D IR imaging to provide a description of spatially resolved metabolic activity at single cell level, finally drawing general conclusions on the implications of these results in SCP.

Experimental Section

Cell Culture

A549 cells (Human Caucasian Lung Carcinoma; ECACC Catalogue Number 86012804) were cultured directly on CaF₂ windows in Dulbecco's Modified Eagle Medium (DMEM) high glucose 4.5mg/ml, no pyruvate, containing sodium bicarbonate (3.7 g/l) and supplemented with 10% foetal bovine serum and 1% Penicillin-Streptomycin antibiotic. Cultures were kept at 37°C with 5% CO₂ in an incubator saturated with water vapour. The initial culture medium was replaced with a fresh medium after 33 hours and the cells in exponential growth phase were allowed to grow for an additional 1 hour before using for metabolic analysis. For FTIR spectromicroscopy measurements the cell-coated window (final cell coverage 40-60%) was transferred to a custom-built solution sample holder kept at 37°C.

Sample Holder for FTIR Imaging on Cells.

The sample holder is a variation of a sandwich design with two optical windows separated by a spacer and has been described previously.¹⁸ A 15 µm gold-coated metal spacer is used to avoid damaging the cells. The temperature of the sample holder is controlled by the thermostatic fluid from a circulating bath. The cells are grown on an optical window as described above. Prior to the experiment the cell coated window is placed into the holder with the growth medium. The spacer is superimposed and the second window is placed on top of the stack, followed by gentle tightening. No perfusion of the sample is performed to ensure the build-up of hypoxic conditions.

Beamline Setup

IR experiments were performed at MIRIAM beamline B22 of the Diamond Light Source, using a Hyperion 3000 microscope coupled to a Vertex 80v interferometer (Bruker UK, Coventry). A summary of beamline parameters and performances for diffraction-limited FTIR microanalysis can be found in reference²⁵.

Synchrotron based IR images and microspectra were acquired on the upstream IR microscope by means of a liquid N₂ cooled FPA photovoltaic MCT detector 64x64 pixels. By using a 36x objective and a 20x condenser optics in transmission mode, similarly to the work described in reference²⁶, the corresponding field of view is circa 70x70 µm². A broadband KBr beamsplitter and a Ge filter provide the mid-IR range up to 4000 cm⁻¹, while the detector cut off was 950 cm⁻¹, as per current FPA technology.

FTIR Measurements

Single channel spectra were obtained by performing a Fourier Transform of the interferogram after apodization with a Blackman-Harris 3-Term function, using a zero-filling factor of 2 and a Power phase correction mode.

A background single channel measurement was performed on a portion of DMEM without cells. The IR beam was then moved to the location of a cell cluster, for the sample single channel measurements described below. 512 scans were averaged for sample and background measurements. Sequential measurements were recorded at 10 min intervals. Pixel response was averaged according to a 2x2 binning scheme.

Spectra are reported as differences from the first measurement in each pixel location and converted to their second derivative by using 13 points Savitzky-Golay smoothing. IR images are built by mapping the distribution of the peak of the second derivative for bands of interest. All data processing and image construction are performed using OPUS 7.1 from Bruker Optics (Ettlingen, Germany).

2D-Correlation Spectroscopy.

2D Correlation Spectroscopy (2DCOS) was introduced as a method to quantify and parametrize the relationship between spectral properties that vary as a function of time or other physical quantity.²⁷ The algorithm involves calculation of the correlation function of the evolving spectral profiles followed by application to the latter of a 2D Fourier transform algorithm. The result is a complex function of two wavenumber variables. The real component is called the synchronous plot, and the imaginary component is called the asynchronous plot. The synchronous plot represents correlations between pairs of wavenumbers that are changing fully in phase or with opposite phase. Two peaks that change in phase have positive “correlation peaks” in the synchronous plot, on both sides of the diagonal. Peaks that change with opposite phase have negative correlation peaks. The asynchronous plot represents correlations between pairs of wavenumbers that have an out-of-phase relationship.

Bands from the same molecule must change perfectly in phase, with positive correlation peaks in the synchronous plot no correlation peaks in the asynchronous plot. The correlation properties of spectral changes arising from the same molecule allow us to assign the full set of bands belonging to that molecule. These properties are the basis of Correlated Cellular Spectromicroscopy (CSM) for the analysis of reactions in living cells.¹⁸

Results and Discussion

The application of CSM to metabolic turnover in hypoxic A549 cells has recently allowed us to identify several metabolites involved in glycolysis, including the end product of fermentation, lactate.¹⁸ We are now building on this work by expanding these results into the second dimension and reconstructing the distribution in space of metabolite formation around individual cells.

By using FTIR imaging with a focal plane detector and a synchrotron light source we are able to track the distribution of metabolite formation in a cluster of hypoxic A549 cells adherent on a CaF₂ optical window. To maximize the spectral quality (figure of merit signal-to-noise ratio or s/n), we performed IR imaging experiments using MIRIAM beamline B22 at Diamond Light Source. The advantage of using a bright synchrotron source and coupling it to a two-dimensional FPA detector consists in a more effective illumination for full field IR imaging at high magnification.²⁸ More specifically for the MIRIAM beamline optics, the 36 \times objective demagnifies the 40 μm FPA pixel to an effective size of $\sim 1.1 \mu\text{m}$ at the sample, and the theoretical signal gain expected per pixel is 20 times with respect to a broadband conventional IR source like a global. Recent experimental work at this beamline²⁶ showed an overall IR signal gain up to 6 times per FPA pixel on living cells in a 10 micron water layer. Noteworthy, the specific beamline design and multiple optics systems allow an effective illumination of the FPA detector within the microscope specification for spectroscopy (illumination variation within 50% of the peak intensity on the area). An additional difficulty that can be addressed by synchrotron based IR imaging is to overcome the strong background due to an aqueous sample environment. This is very challenging for IR spectroscopy because of the strong absorption from water that causes a significant throughput reduction. In the optical configuration used for these experiments, synchrotron illumination gives a clear advantage in terms of increased photon flux density relative to the global, which allows enough signal at single pixel level for proper absorption calculation, including water correction and second derivative analysis. In so doing, we follow an approach that has already proven useful in identifying the metabolic turnover of isotopically labelled water molecules by functional fibroblasts.²⁶

Cells are enclosed in the chamber of the sample holder and brought to the IR microscope for measurement while maintaining a temperature $T = 37 \text{ }^\circ\text{C}$. No flushing of the cell with medium is performed after sealing, thus allowing the establishment of hypoxic conditions. A background

measurement is performed on a region of the chamber where only medium is present. The field of view is then moved to a group of cells where spectra are measured sequentially.

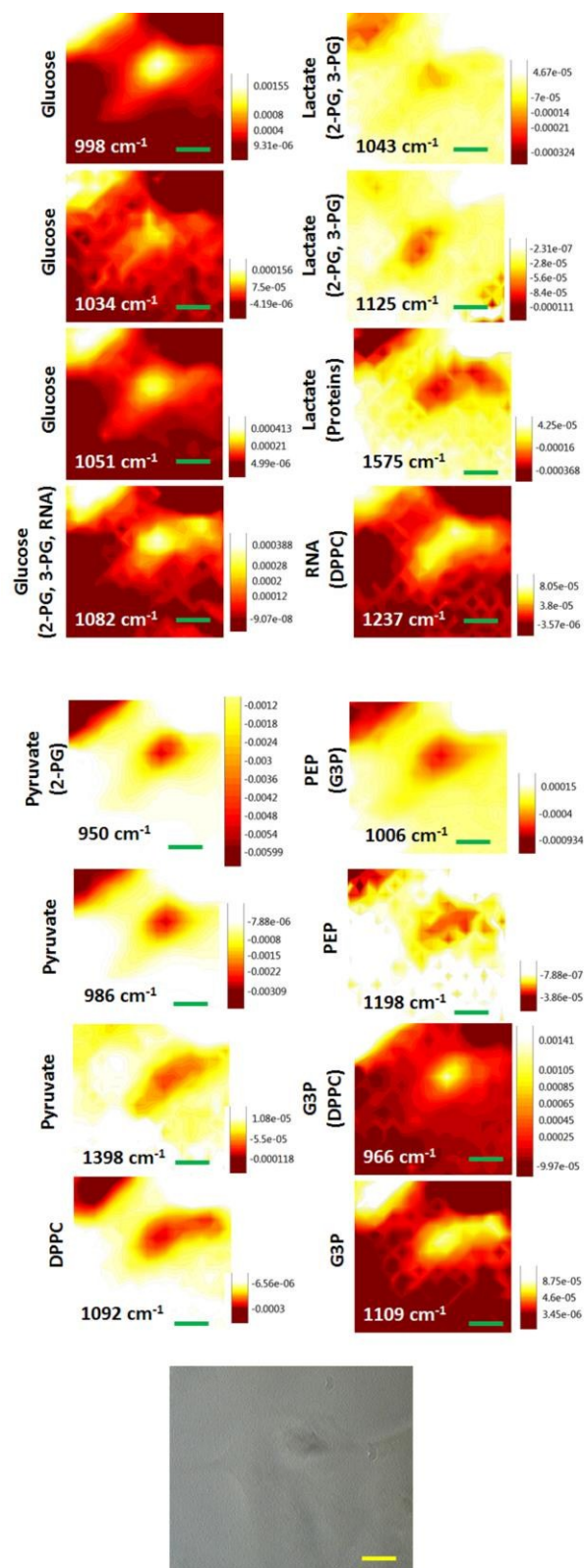


Figure 1. IR images from a cluster of A549 cells at different wavelengths. Images show the distribution of the second derivative peak of specific absorption bands. Spectral images are reported as differences from the first image, recorded 50 min after the beginning of the measurement. The maps correspond to selected absorption bands associated to specific molecules involved in glycolysis. Each map includes the assignment to a specific molecule as determined in reference ¹⁸. The presence of overlapping bands from other molecules is represented by listing in brackets the molecules giving rise to the overlap. Inset: visible image of the cell cluster collected soon after these IR images.

Figure 1 shows the visible light transmission image of a cluster of A549 cells (inset) and the corresponding distribution of several absorption bands throughout the cluster. The bands were recorded as difference of absorption from the beginning of the measurement. The maps in Figure 1 correspond to the total variation over a 50 min interval. The maps were constructed by plotting the intensity of the 2nd derivative of absorption at the given wavenumber. Assignments to bands of specific molecules are based on the CSM analysis of this cellular system under identical conditions.¹⁸ The vertical scale of each map has been expanded differently to enhance visibility of the distribution of interest.

The periphery of the full field of view is not usable because of the low light intensity that illuminates the detector. This is due to the inhomogeneous illuminations of the sample when using the synchrotron light source. The light source was aligned to increase flux in the central portion of the detector, while excluding the periphery. Images have been cropped relative to the original size to exclude most of the unusable regions from the field of view. Despite this, some portions of the cropped image still display high noise levels and high apparent baselines and are of little use for a sensitive measurement. These regions correspond to the corners of the image and are generally sent out of scale when adjusting the intensity interval to be displayed.

It is immediate apparent from Figure 1 that changes in metabolite absorption are observed in space and in time. Most of the changes are localized in the proximity of one large cell in the upper centre of the map and give rise to clear gradients around this cell. Another location where a clear concentration gradient is observed is the upper left corner of the map, because of the presence of other cells located at the very edge of the field of view. Other cells are seen in the lower half of the image, but without any detectable concentration gradients. It is notable that the latter are seen shifting their location during the course of this measurement, thus confirming their viability.

The high level of smoothing associated to the Savitzky-Golay algorithm, 13 points, is required for extracting the weaker spectral changes from the noisy baseline and allow mapping. However, this improvement comes at the cost of spectral resolution. Several overlapping bands cannot be resolved and some of the maps in Figure 1 must be assigned to spectral contributions from more than one molecule. Specific cases of overlap are highlighted both in the figure and in the text. Presently, the need to decrease spectral resolution to compensate for a low s/n ratio is the main drawback in the application of IR imaging to metabolic analysis *in vivo*. In comparison, spectral analysis by CSM in a sample larger than 50x50 μm can be performed by using 7 or 9 smoothing points in the Savitzky-Golay algorithm.¹⁸

Some discrimination is possible between events occurring in the exterior and in the interior of the cell, although only on a qualitative basis. The presence of headspace between the top of the cell and the upper optical window means that some contribution from components of the medium is present in every measurement location and cannot be separated without accurate knowledge of the topography of the cell.

Gradients in space are observed for bands identified by CSM. Glucose and lactate provide the strongest contribution to the spectral variations and the associated maps. This is in agreement with their role as substrate and final product of glycolysis and fermentation. In the case of lactate, maxima in the concentration gradients for all bands are observed both in the central part of the cell and in its periphery, extending into the extracellular space. This is expected since lactate is known to be released by the cell into its surroundings. In contrast, glucose bands show

a negative gradient, with a minimum of concentration only in the central region of the cell. This is also expected since glucose is consumed within the cytoplasm. Glycolysis is fully catalysed by enzymes that are distributed in the cytoplasm itself, as opposed to oxidative phosphorylation, which is localized in the mitochondria. Therefore the drop in glucose concentration is expected to track the volume of cytoplasm that is probed by the beam. The quality of the cellular image in the inset of Figure 1 is degraded by chromatic aberrations introduced by the optical windows, preventing us from making an accurate comparison. Nonetheless, this is at least qualitatively confirmed by comparison of maps from glucose bands at 998 cm^{-1} , 1034 cm^{-1} and 1051 cm^{-1} (which do not include major overlap from other bands) and with the visible light image. Glucose gradients track the topography of the cell and appear negligible outside of the cell. The implication is that cellular uptake, as opposed to diffusion or enzymatic degradation, is a rate limiting step in glucose consumption.

One interesting observation is the presence of clear gradients associated to bands that were only weakly detected in extended clusters of A549 cells under identical conditions.¹⁸ Such metabolites include pyruvate, phosphoenolpyruvate and the phosphoglycerates. All of them are present at absolute concentrations within the detection limit of IR spectroscopy, and have been observed in macroscopic measurements of metabolic turnover, for example in yeast lysates.²⁹ The lack of spectroscopic evidence of these species in the difference spectra from A549 cell clusters was attributed to steady state conditions that maintain the concentration of intermediate metabolites relatively stable throughout the cluster. Under these conditions only reactants and final products are observed in difference spectra. Intermediate species are observed only as far as they are displaced from homeostasis by a transient perturbation.¹⁸ In the latter measurements, concentration changes are averaged over the whole portion of the sample. In contrast, in the current imaging measurements the local concentration of a molecule varies in response to both local turnover and diffusion, making it easier to avoid steady state conditions. The resulting concentration gradients extend in space and also change over time, facilitating detection of intermediate species compared to an averaged bulk measurement.

Spectromicroscopy measurements on cell clusters¹⁸ failed to detect appreciable changes in concentrations of ATP and inorganic phosphate (PO_4), despite the fact that the absolute cellular concentrations of these molecules are well within the detection limits of the technique. Imaging measurement for this work also fail to detect any unequivocal contributions from these two species. No gradients can be observed for the strongest absorption band specific to aqueous ATP, at 1075 cm^{-1} , nor for the strongest absorptions from PO_4 at pH close to neutral, at 1077 cm^{-1} and 1159 cm^{-1} . The reasons for this absence are not clear. It is known from bulk measurements that cellular variations in ATP concentration are very rapid following perturbation of a system³⁰ and a stationary state is rapidly reached. Nonetheless, the absence of observable concentration gradients in space is surprising. Possible explanations will be tested in future experiments. One possibility is that the spectra of these species in the cellular environment differ from those of the species in bulk aqueous solution. Complexation to H-bonding donors or to metal ions can shift vibrational transitions by a few up to tens of wavenumber units. In this case we would need to identify the correct spectral bands for the cellular forms before being able to locate them in cellular spectra and maps. An alternative or additional possibility is that the intracellular localization of these species prevents the formation of gradients driven by passive or active transport across the cellular membrane. The combination of this effect with the rapid achievement of steady state conditions would prevent the observation of concentration changes in the present experiment. Nonetheless, the latter explanation would be surprising given current understanding of PO_4 and ATP transport.

Current results confirm that the detectability of small molecules in cellular spectra is viable. In an attempt to generalize this conclusion and encourage the design of future experiments we have searched available information about small molecules that are potentially identifiable in an FTIR experiment. Table 1 summarizes the results of a search performed in the Human Metabolome Database ³¹ (HMDB), maintained at the University of Alberta, Canada (www.hmdb.ca). The table lists the cytoplasmic concentration values listed at the HMDB for several human metabolites. Each entry is the outcome of measurements from a specific publication. The specific HMDB entry provides a link to the original publication and corresponding information about the method, source cell type, data analysis and associated uncertainties. The table lists only the most concentrated metabolites, expected to be detectable in an FTIR bulk measurement. For the current detection limit we tentatively take the value of 20 μM , recently reported by Chan *et al.* ³² Detection limits with a microscopy configuration are expected to be correspondingly worse, depending on aperture size, optical configuration and light source. Due to the variability and limited selection of cell type, sample preparation, and analytical method, Table 1 is not meant to represent the composition of any real cellular state. It is rather a general guide to what specific molecules are potentially accessible to investigation with an FTIR spectroscopy or microscopy measurement. The list of entries is expected to increase in the future, as accurate cytoplasmic concentrations of more metabolites are reported. One outstanding absence is the concentration value for phosphate species, which is currently being debated, but which is expected to be at upper end of the table. The detection limit is also expected to shift to lower values as the sensitivity of FTIR and other IR spectroscopic methods is improved.

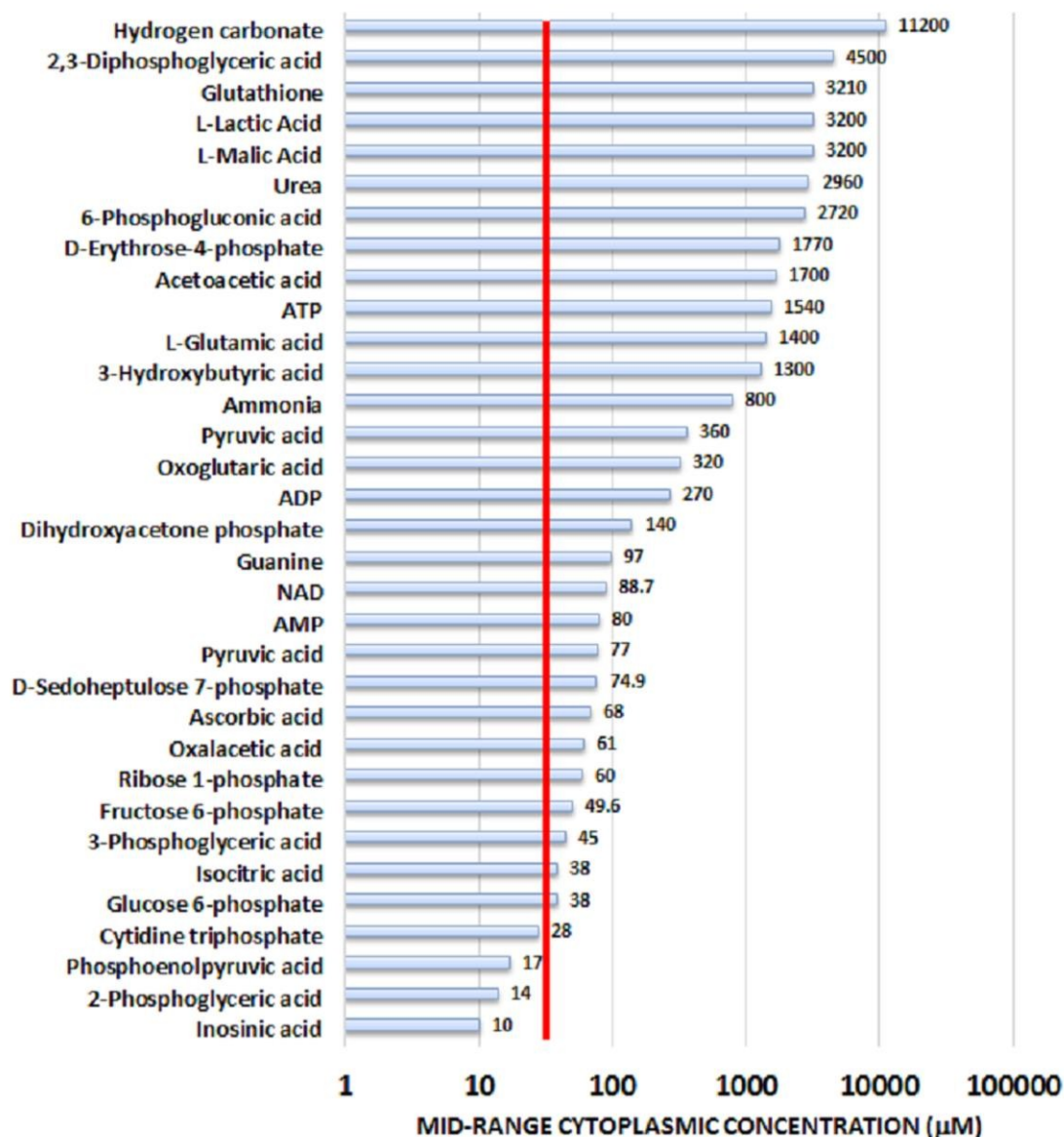


Table 1. Reported cytoplasmic concentrations of human metabolites from the Human Metabolome Database (HMDB). The red line shows a recently reported limit for the detectability of a small molecule in an FTIR measurement.³²

Table 1 shows that only a small fraction of known human metabolites, of the order of 1%, is detectable. Despite the low percentage value, in absolute terms this corresponds to at least 30 molecular species. The spectral complexity associated even to this relatively modest set is daunting, when considering that $3N-6$ (N = number of atoms) vibrational normal modes are associated to each molecular species, even if not all of them are observed in an absorption experiment. In this respect, the use of techniques like CSM, including isotopic substitution experiments, will prove critical in mining the wealth of biochemical information associated to cellular and tissue sample.

One important consideration is that the spectral contribution of individual metabolites varies from cell to cell. It is expected to depend on all the factors that influence the cellular metabolic state, including the phase of the cell cycle, the cellular environment and the availability of nutrients. A related consideration is the verification that several of these molecules are not a stable complement of the cell, but are constantly and exchanged with the medium and with adjoining cells over the scale of a minutes and seconds. This is unlike the complement of macromolecules that on average are subject to slower turnover. The immediate consequence of these observations is that the spectroscopic properties of a cell (we are talking about IR absorption spectroscopy but this could apply to Raman spectroscopy as well, and to other vibrational spectroscopy techniques) are dependent on how the cell has been interacting with its surroundings shortly before its spectroscopic probing. The properties of the surrounding medium, the local temperature and the level of cellular confinement are of course all obvious and major factors in determining the metabolic complement of the cell which is probed by a spectromicroscopy experiments. However, many other factors are also affecting the composition of the system, such as the shape of the cell relative to the confocal aperture used for the measurement (which determines the ratio of cellular volume to medium volume which is present in the spectra), the flow rate of the medium in a microincubator, the diffusion rate of the various nutrients through the sample, the retention time of the cell in a sampling loop or sampling capillary while being transferred during a biopsy, the delay in the transfer of a cell from one holder to another, the duration of a centrifugation or filtration step during cellular harvesting, the method and skill of the executor of a biopsy in separating a cell from its surrounding tissue, etc. All these innumerable factors can affect the resulting complement of small molecules of a cellular sample, while they have little effect on the contribution of major macromolecular components, which are more stably associated to the cell and show less variability in relative concentration. Many of these factors can be reproducibly controlled when operating *in vitro*, e.g. when comparing the spectra of cell lines cultivated under identical conditions and using the same sample holder. This variability is also much less appreciated when working on tissue sections. Most sections are obtained from biopsies or tissue harvest that are immediately followed by cryopreservation, fixation and/or sectioning. This ensures that the complement of metabolites of the tissue is either fully retained with appropriate spatial distribution (as in cryosectioning) or is lost in a reproducible way (as in fixation followed by sectioning). The possibility to control the loss of metabolites is one likely reason for the early success of SCP applications based on the analysis of tissue sections. However, major variability is expected when comparing cellular samples of different origin and measured in different laboratories. Loss or variation of the metabolite complement of single cells is difficult to control and this uncertainty will be the main barrier in developing reliable diagnostic applications for SCP in a clinical setting, where small procedural variations are expected between laboratories, between different practitioners and between different operations of the same practitioner.

Conclusions

By performing time resolved and spatially resolved measurements of cellular systems we have observed and identified a number of small molecule metabolites in A549 cells maintained under hypoxic conditions. This work demonstrates the viability to use CSM and IR imaging with synchrotron radiation to study metabolic turnover with single cell resolution.

To our knowledge, IR imaging is the first technique that allows discriminating cellular metabolic production in a non-destructive way, retaining cellular function, with single cell resolution. These results open the way to the use of IR imaging in a CSM analysis scheme to perform specific studies of the biochemistry of individual cells in multicellular systems.

Techniques for the co-culture of different cell types and the use of organotypic cultures can allow extension to systems of increased complexity. The role of fluctuations of local concentrations in metabolic networks and the interaction between metabolic activities in adjoining cells can all be measured and hypothesis tested.

One potential offshoot is the use of the technique to assess the activity of compounds of pharmacological interest in multicellular assemblies that act as models for more complex living organs. Local compound turnover, partition between different cell types and intracellular exchange of metabolic products can all be tested, qualitatively and quantitatively, in an IR imaging experiment and analysed by CSM.

An additional direction for future development is the transfer of the CSM approach to other spectroscopic techniques that provide correspondingly rich and complex spectra of cellular samples. Raman spectromicroscopy and imaging is the obvious first candidate, being also a vibrational spectroscopic technique.³³ However any set of spectroscopic data can be potentially analysed using a 2DCOS approach, including the ones based on UV/vis and x-ray photon absorption and scattering.²⁷ One appealing development will be the integration of different techniques into a single approach that follows the CSM scheme. The resulting multispectral method would be more than the sum of its parts. Correlations between widely separated spectral regions may help to associate electronic and vibrational transitions to the same molecule. A correlation approach that involved both IR and Raman spectra would be especially powerful. It would take advantage of the complementary selection rules for the two techniques to provide more solid band assignments and more accurate identification of molecules.

The main limitations are the ones that generally affect all experiments of IR Spectromicroscopy and imaging. One disadvantage is the relatively short penetration depth of mid-IR radiation in tissue, of the order of 10-50 μm , depending on the specific spectral interval, which restricts most experiments to single or double cellular layers. The second disadvantage is the limited sensitivity which, despite the extensive list of detectable molecules presented in Table 1, still excludes that vast majority of metabolites. Concerning the latter aspect, an increase in the sensitivity of 2D-COS based methods, such as CSM, is obtained because of the reduced noise contributions in synchronous plots,³⁴ although the improvement has not been quantified yet.

The present work confirms that the detectability of small molecules in IR cellular spectra is far from being an exception. It is rather the rule. Although in absolute terms their contribution is often smaller than that of the canonical components of cellular spectra, it is far from negligible. Future work on cellular and tissue IR spectra aiming at molecular characterization of the sample will need to keep the contribution from small molecules into consideration and conclusions from past work that neglected this contribution should be reassessed.

Acknowledgements

We are grateful to Prof. Frank Martin, Lancaster University, and Dr. Endre Laczko, Functional Genomics Centre Zurich, for helpful discussion, and to Blagoj Sarafimov, Paul Scherrer Institute, for construction of the sample holder. Some of the authors (LQ and TZ) acknowledge Diamond Light Source for beamtime allocation at the MIRIAM beamline, B22, (proposal SM12221) and support, which contributed to the results presented here.

References

1. P. Dumas and L. Miller, *Vib. Spectrosc.*, 2003, **32**, 3-21.
2. M. Diem, A. Mazur, K. Lenau, J. Schubert, B. Bird, M. Miljkovic, C. Krafft and J. Popp, *Journal of Biophotonics*, 2013, **6**, 855-886.
3. P. Lasch, J. Kneipp and D. Naumann, *Spectroscopy of Biological Molecules: New Directions*, 1999, 509-510.
4. D. C. Fernandez, R. Bhargava, S. M. Hewitt and I. W. Levin, *Nat Biotech*, 2005, **23**, 469-474.
5. G. Bellisola and C. Sorio, *American Journal of Cancer Research*, 2012, **2**, 1-21.
6. L. Martin Francis and J. Fullwood Nigel, *Proc Natl Acad Sci U S A*, 2007, **104**, E1.
7. L. Quaroni and T. Zlateva, *Analyst*, 2011, **136**, 3219-3232.
8. J. R. Mourant, R. R. Gibson, T. M. Johnson, S. Carpenter, K. W. Short, Y. R. Yamada and J. P. Freyer, *Physics in Medicine and Biology*, 2003, **48**, 243-257.
9. N. Holman Hoi-Ying, A. Bjornstad Kathleen, P. McNamara Morgan, C. Martin Michael, R. McKinney Wayne and A. Blakely Eleanor, *J Biomed Opt*, 2002, **7**, 417-424.
10. M. Romeo, C. Matthaus, M. Miljkovic, S. Boydston-White and M. Diem, *Biomedical Vibrational Spectroscopy and Biohazard Detection Technologies*, 2004, **5321**, 124-129.
11. M. K. Kuimova, K. L. Chan and S. G. Kazarian, *Appl. Spectrosc.*, 2009, **63**, 164-171.
12. P. Heraud, J. Beardall, D. McNaughton and B. Wood, *Phycologia*, 2005, **44**, 104.
13. M. J. Nasse, S. Ratti, M. Giordano and C. J. Hirschmugl, *Applied Spectroscopy*, 2009, **63**, 1181-1186.
14. L. Quaroni, T. Zlateva, D. Bedolla, S. Massaro and V. Torre, *ChemPhysChem*, 2008, **9**, 1380-1382.
15. L. Quaroni, T. Zlateva and E. Normand, *Analytical Chemistry*, 2011, **83**, 7371-7380.
16. D. Ami, A. Natalello, M. Lotti and S. M. Doglia, *Microbial Cell Factories*, 2013, **12**.
17. L. Chen, H.-Y. N. Holman, Z. Hao, H. A. Bechtel, M. C. Martin, C. Wu and S. Chu, *Analytical Chemistry*, 2012, **84**, 4118-4125.
18. L. Quaroni and T. Zlateva, *Analytical Chemistry*, 2014, **86**, 6887-6895.
19. D. I. Ellis, G. G. Harrigan and R. Goodacre, *Metab. Profiling*, 2003, 111-124.
20. M. J. Baker, J. Trevisan, P. Bassan, R. Bhargava, H. J. Butler, K. M. Dorling, P. R. Fielden, S. W. Fogarty, N. J. Fullwood, K. A. Heys, C. Hughes, P. Lasch, P. L. Martin-Hirsch, B. Obinaju, G. D. Sockalingum, J. Sule-Suso, R. J. Strong, M. J. Walsh, B. R. Wood, P. Gardner and F. L. Martin, *Nature Protocols*, 2014, **9**, 1771-1791.
21. M. Diem, S. Boydston-White and L. Chiriboga, *Appl. Spectrosc.*, 1999, **53**, 148A-161A.
22. L. M. Miller and P. Dumas, *Biochim. Biophys. Acta, Biomembr.*, 2006, **1758**, 846-857.
23. M. Z. Kastyak, M. Szczerbowska-Boruchowska, D. Adamek, B. Tomik, M. Lankosz and K. M. Gough, *Neuroscience*, **166**, 1119-1128.
24. K. L. Goff, L. Quaroni, T. Pedersen and K. E. Wilson, in *Wirms 2009: 5th International Workshop on Infrared Microscopy and Spectroscopy with Accelerator Based Sources*, eds. A. PredoiCross and B. E. Billinghamurst, 2010, vol. 1214, pp. 54-56.
25. G. Cinque, M. Frogley, K. Wehbe, J. Filik and J. Pijanka, *Synchrotron Radiation News*, 2011, **24**, 24-33.
26. L. Quaroni, T. Zlateva, B. Sarafimov, H. W. Kreuzer, K. Wehbe, E. L. Hegg and G. Cinque, *Biophysical Chemistry*, 2014, **189**, 40-48.
27. I. Noda, *Applied Spectroscopy*, 1993, **47**, 1329-1336.

28. M. J. Nasse, M. J. Walsh, E. C. Mattson, R. Reininger, A. Kajdacsy-Balla, V. Macias, R. Bhargava and C. J. Hirschmugl, *Nature Methods*, 2011, **8**, 413–416.
29. T. Mair, L. Zimanyi, P. Khoroshyy, A. Muller and S. C. Muller, *Biosystems*, 2006, **83**, 188-194.
30. F. L. Martin and A. E. M. McLean, *Toxicology*, 1995, **104**, 91-97.
31. D. S. Wishart, C. Knox, A. C. Guo, R. Eisner, N. Young, B. Gautam, D. D. Hau, N. Psychogios, E. Dong, S. Bouatra, R. Mandal, I. Sinelnikov, J. Xia, L. Jia, J. A. Cruz, E. Lim, C. A. Sobsey, S. Shrivastava, P. Huang, P. Liu, L. Fang, J. Peng, R. Fradette, D. Cheng, D. Tzur, M. Clements, A. Lewis, A. De Souza, A. Zuniga, M. Dawe, Y. Xiong, D. Clive, R. Greiner, A. Nazyrova, R. Shaykhtudinov, L. Li, H. J. Vogel and I. Forsythe, *Nucleic Acids Research*, 2009, **37**, D603-D610.
32. K. L. A. Chan and P. L. V. Fale, *Analytical Chemistry*, 2014, **86**, 11673-11679.
33. K. Kong, C. Kendall, N. Stone and I. Notinger, *Advanced Drug Delivery Reviews*, 2015, **89**, 121-134.
34. L. Quaroni and E. Normand, in *Wirms 2009: 5th International Workshop on Infrared Microscopy and Spectroscopy with Accelerator Based Sources*, 2010, vol. 1214, pp. 66-68.